

# Constructing the Next Generation Cryogenic Sapphire Oscillator

C.R. Locke, S. Munro, M.E. Tobar, E.N. Ivanov, G. Santarelli<sup>#</sup>

Department of Physics, University Of Western Australia.

<sup>#</sup> Bureau National de Metrologie-Systemes de Reference Temps Espace, Paris, France.

**Abstract:** - This work describes the next generation cryogenic sapphire oscillator designed and constructed at the University of Western Australia (UWA), for the PHARAO project developed by the Centre National d'Etudes Spatiales (CNES) and BNM-SYTRE (Bureau National de Metrologie-Systemes de Reference Temps Espace.) The oscillator has now been transported and installed in CNES, Toulouse. It will function as the interrogation oscillator of the prototype and space versions of the PHARAO Cs atomic clock, for all pre-launch ground based tests.

## 1. INTRODUCTION

The University of Western Australia's (UWA) cryogenic sapphire oscillator project has been operational since 1988[1, 2]. It is currently the most stable frequency source over integration times ( $\tau$ )  $1 < \tau < 100$  s. [3, 4] Within such sapphire resonators, exceptionally high unloaded quality factors of  $8 \times 10^9$  have been measured[5]. Sapphire's low loss tangent may be exploited by selecting a highly confined, high order resonant mode [6]. During 2000, a fractional frequency stability of  $2.4 \times 10^{-16}$  was demonstrated at an integration time of 32 s. The oscillator was based on a sapphire resonator operating on a  $H_{14,1,6}$  (WGE) 11.9 GHz Whispering Gallery (WG) mode at a temperature of 6K.

The performance of atomic fountain clocks has conventionally been limited by the performance of the local oscillator, which regulates the time between launched atoms [7]. The goal of this project is to provide a secondary frequency standard with fractional frequency stability better than  $10^{-14}$  at integration times of 1 to 10 seconds. It is to be used as a "fly-wheel" oscillator for ground based tests of PHARAO. One can meet this requirement using a liquid helium cooled sapphire resonator [8]. The construction can be divided into two parts, the resonator, and the oscillator.

The resonator needs to have a well-defined intrinsic frequency, and to be stable at this frequency. For good short-term stability we need the maximum possible quality factor (Q-factor), and for good medium term stability we need good isolation from environment (vibration and temperature). The resonator must have low sensitivity to temperature fluctuations; in order to reduce the requirements of a temperature control system, we use a resonator that has a turning point in its frequency/temperature dependence.

## 2. THE RESONATOR

We use high quality HEMEX sapphire as a resonator. Sapphire satisfies many of the criteria listed above; single crystal sapphire at cryogenic temperature (4~10K) has low defect density, low microwave loss (high Q), a high Young's modulus (vibration and tilt sensitivity reduced), small thermal capacity and high thermal conductivity (easier temperature control.)

We utilize high quality factor (Q-factor) WG modes that have a high azimuthal number to improve electromagnetic confinement, which reduces the conductor loss of the cavity. The construction of the cavity is shown in figure 1. Previously, a double-spindle sapphire resonator was at the heart of the cryogenic oscillator. The crystal was grasped top and bottom by copper sheaths within the niobium cavity. Long-term frequency drifts were observed, and the resonant frequency was irreproducible on thermal cycling. These difficulties were attributed to a combination of creep and mechanical stress induced by the rigid mounting assembly[4]. To combat this problem, a single spindle crystal has been implemented which is supported only from below.

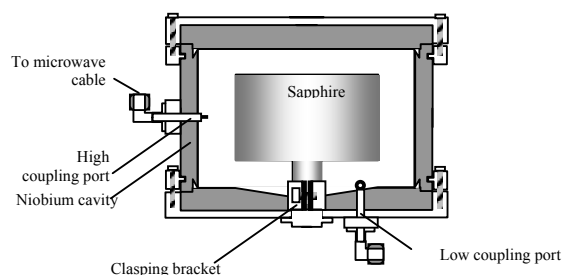


Figure 1. Sapphire and cavity

Shown in figure 2 is the inner can and outer can. The niobium cavity encasing the sapphire resonator is immersed in a helium bath (~4K) to reduce thermal noise and increase the Q-factor of the resonance. The helium bath is shielded from the environment by a heavily insulated dewar approximately 1.8m high and 0.5m wide. The sapphire itself is attached to the lower end of an insulating stainless steel "insert" which is placed into this dewar. The insert consists of a series of baffles to reduce convection and maintain temperature within the dewar. Stainless steel microwave transmission lines are used to complete the room temperature

to liquid helium section of the oscillator circuit due to their low thermal conductivity. To prevent stress on the microwave fitting associated with thermal cycling, loops are placed within the microwave cables.

While it is important to maintain the resonator at helium temperatures, it is also important to thermally isolate it from the surrounding helium bath to reduce the severity of any temperature fluctuations. As such, the niobium cavity is contained within an “inner can” turbo pumped to  $\sim 10^{-6}$  Torr at room temperature, and then further cryopumped upon cooling. Heat is extracted from this inner can via the copper-mounting shaft. The inner can is contained within a second “outer can” which is pumped to  $\sim 10^{-3}$  Torr to reduce thermal conduction into the dewar and also to provide a vacuum environment for the microwave components, which sit inside the can. Heat is drawn from the outer can via three copper heat sinks, which sit in the helium bath.

A heater wire is situated on the copper post inside the outer can to maintain the sapphire at its turning point in the frequency/temperature dependence (around 7K). Figure 3 shows the measured frequency-temperature turning point. Calibrated Carbon-Glass and Germanium RTDs situated on the copper post in the outer can were used to measure the temperature. We measure a turning point at around 7.5K. This is due to  $Ti^{+3}$  and  $Mo^{+3}$  ions. We calculate a curvature of  $3 \text{ Hz K}^{-2}$ . To achieve fractional frequency stability of  $10^{-16}$  at 1 mK offset from the turning point, need 0.3mK temperature stability. Using a commercial temperature controller, fractional frequency stability around the  $10^{-15}$  level can be expected.

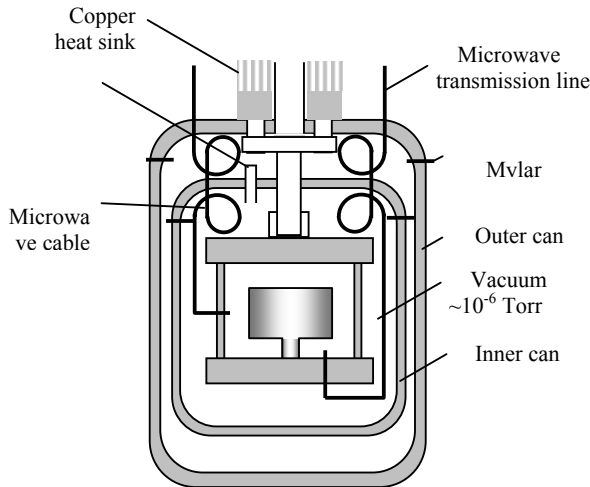


Figure 2. The inner and outer can construction

Previously, there were problems experienced with creating vacuum seals. The seals were achieved by crushing indium wire within a tongue and groove. Leaks were common and difficult to find, and the whole process needed to be repeated when thermally cycling the experiment. A new Mylar seal system was developed which may be used repeatedly. Using this design, it was possible to make all microwave and wiring feed-throughs as modular units for ease of assembly and to

allow more flexibility with placement. The new seals were found to be most effective and no leaks have been detected in any of the seals implemented.

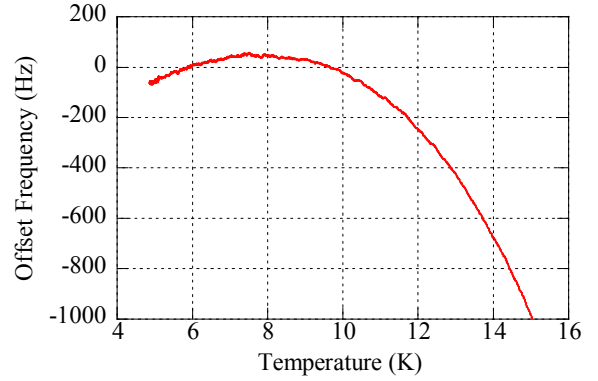


Figure 3. Frequency-temperature turning point

The inner can itself was redesigned as a smaller, lighter unit. A rounded bottom maintains structural rigidity while allowing for thinner walls. It also reduces the amount of liquid helium required to initially cool the can.

### 3. COUPLING COEFFICIENT

The coupling coefficient ( $\beta$ ) is a measure of the fraction of incident power which is absorbed into the resonator. It may be calculated explicitly by interrogating the resonator in reflection, and calculating the ratio of reflected power on resonance ( $P_{on}$ ) to the reflected power off resonance ( $P_{off}$ ). The coupling coefficient is then given by:

$$\beta = \frac{1 - \sqrt{P_{on} / P_{off}}}{1 + \sqrt{P_{on} / P_{off}}} \quad (1)$$

It is desirable to have unity coupling (i.e.  $P_{on} = 0$ ) on the input probe. This minimizes the reflected signal, improving secondary noise effects such as the conversion of spurious amplitude modulation (AM) to phase modulation (PM) within the oscillator. The output probe coupling affects the input probe coupling. To minimize this effect, it is set to be less than unity. An output probe coupling of  $\sim 0.1$  is a reasonable compromise, such that the loop oscillator does not require too much gain to overcome coupling losses.

Upon cooling the resonator, the quality factor ( $Q$ ) and coupling coefficient ( $\beta$ ), to reasonable approximation, increase proportionately. The relationship between coupling and quality factor at room and cryogenic temperatures is given by.

$$\frac{Q_{300K}}{Q_{4K}} = \frac{\beta_{300K}}{\beta_{4K}} \quad (2)$$

The  $H_{14,1,8}$  mode has a room temperature Q- factor of  $\sim 10^5$ . Based on previous performance of pure sapphire cryogenic resonators one may expect this factor to increase to  $\sim 10^9$  at 4K. Thus, to attain unity coupling at cryogenic temperatures, the coupling should be set to  $\sim 10^{-4}$  at room temperature (actually  $2 \times 10^{-4}$ ). Similarly, the low coupling port ( $\beta_{4K} = 0.1$ ) should have room temperature coupling of  $\sim 10^{-5}$  (actually  $2 \times 10^{-5}$ ).

The coupling was set optimally after a series of iterative cooldown cycles. Shown in figure 4 is the operation mode at 4K in reflection. The frequency is the  $H_{14,1,8}$  mode at 11.931, 819 GHz. The Q-factor is approximately  $2 \times 10^9$ , and the coupling is around 0.7.

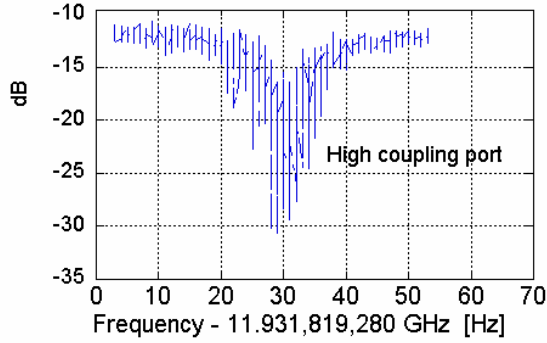


Figure 4. Mode characteristics at 4K.

The low coupling port was also measured in reflection to be 0.1.

### 3. THE OSCILLATOR

The functionality of the helium clock relies on the ability of the oscillator circuit to lock to an appropriate resonant mode within the sapphire. A mode's resonant frequency is dependent on both temperature and power. Temperature changes in the cryogenic environment alter both the physical dimensions and permittivity of the resonator. The frequency dependence on power is largely due to the mechanical distortion of the sapphire body from the pressure of the stored electromagnetic radiation. There are also intrinsic noise sources within the oscillator largely due to fluctuations in the active circuit elements, while external factors such as temperature, mechanical stress and vibration can induce further noise within the oscillator circuit. It is the role of the control system to minimize these noise sources in order to maintain a tight frequency lock of the oscillator to a stable mode within the resonator.

The control systems required are ;

- i. Frequency control system to lock oscillator frequency to resonator frequency
- ii. Reduction of spurious AM created due to phase modulation
- iii. Power control servo

We describe each of these systems in detail.

#### i. Frequency control

We use tunnel diode detectors in the temperature stable cryogenic environment (in the outer can.) Shown in figure 5 are the noise floors of the lock-in amplifier, detector and integrator. This level will tell us the gain required in Pound locking circuit

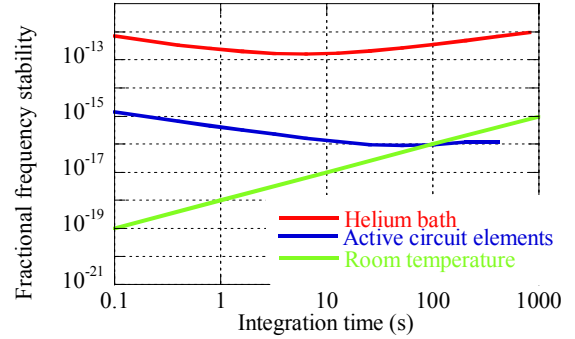


Figure 5. Noise floor due to electronic components and helium bath level fluctuations.

This gain can be provided by using a low gain lockin amplifier with sensitivity setting of 5mV for 10V output, and time constant  $\tau \sim 1\text{ms}$ , followed by a high gain integrator.

#### ii. Spurious amplitude modulation

The control system implements two voltage controlled phase shifters (VCPs) (one for phase modulation, and one for phase correction.) The phase modulator is required for frequency discrimination. In previous designs, this component is biased by the AM servo to ensure that  $dK/dV$  is zero to first order (where K is the amplitude transfer function and V is the bias voltage). This system is reliant on the existence of such a turning point at some bias voltage and a given resonant frequency. While some VCPs do exhibit this behavior, it often occurs at higher bias voltages, where the efficiency of the VCP ( $d\phi/dV$ ) is compromised. Ultimately, it is desirable to have  $d\phi/dV = \max$ ,  $dK/dV = 0$ .

There is inherent difficulty associated with finding VCPs with maximum voltage-phase conversion efficiencies at a bias voltage where there is zero voltage-gain conversion. This problem is particularly significant if the operator desires to lock to different modes within the resonator, as a different VCP must be found. A novel AM servo was produced which does not rely on a turning point in the voltage response of the gain in the VCP. By injecting antiphase AM into the loop, the control system effectively creates a turning point for the VCP at a particular bias voltage. The control system then maintains this bias voltage such that the VCP continues to operate at this optimum bias.

The measured voltage noise with the AM control system on is shown in figure 6.

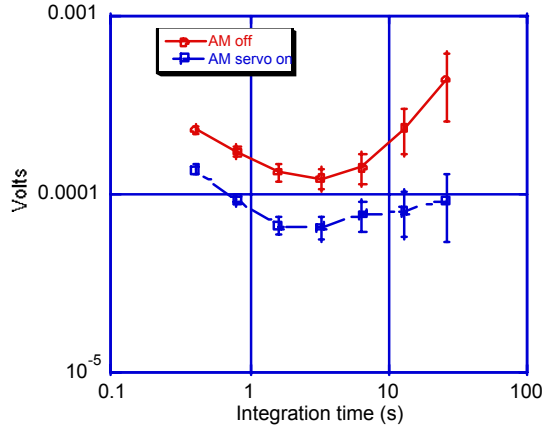


Figure 6. Spurious AM reduction system.

This voltage noise of 0.0001V in figure 6 is equivalent to a fractional frequency stability of  $3 \times 10^{-16}$ .

### iii. Power control system

Dominant effect of power variations is radiation pressure-induced permittivity change in sapphire. This has been previously measured as  $5 \times 10^{-11}$  per mW dissipated [9]. A 20dB directional coupler in the cryogenic environment feeds some of the incident signal upon a detector. This DC voltage is then subtracted from a stable reference, filtered, and fed back into a voltage controlled attenuator to maintain constant power incident upon the sapphire resonator. This control system suppresses fluctuations in power by over 30dB at frequencies DC to 100Hz.

## 4. VOLTAGE NOISE

Shown in figure 7 is the measured voltage noise of the cryogenic oscillator with all control systems active. This measurement is not sensitive to temperature fluctuations (the dominant source of noise) and is only useful in confirming that all controls are working adequately. A digital Voltmeter (DVM) was used to at 0.4 second integration times, and then the Allan Deviation calculated. This Allan Variance of voltage fluctuations ( $\delta_u$ ) was then transformed into fractional frequency stability ( $\delta_f/f_0$ ) at the resonant frequency ( $f_0$ ) via the sensitivity of the frequency discriminator ( $S_{FD}$ );

$$\frac{\delta_f}{f_0} = \frac{\delta_u}{f_0 S_{FD}} \quad (3)$$

where

$$S_{FD} = \frac{10}{\sqrt{2} S N S} K_{amp} \gamma_{det} 2 P_{inc} \frac{2\beta}{(1+\beta)^2} \frac{\varphi_m}{\Delta f_{0.5}} \quad (4)$$

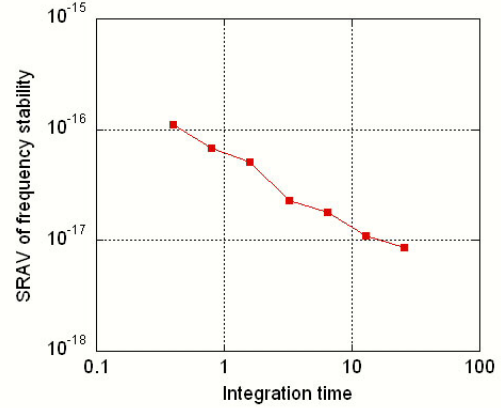


Figure 7. Voltage noise with all control systems operational.

A fractional frequency stability of  $10^{-16}$  at 1s integration time was measured. The operational clock was then compared against a maser, as shown in figure 8.

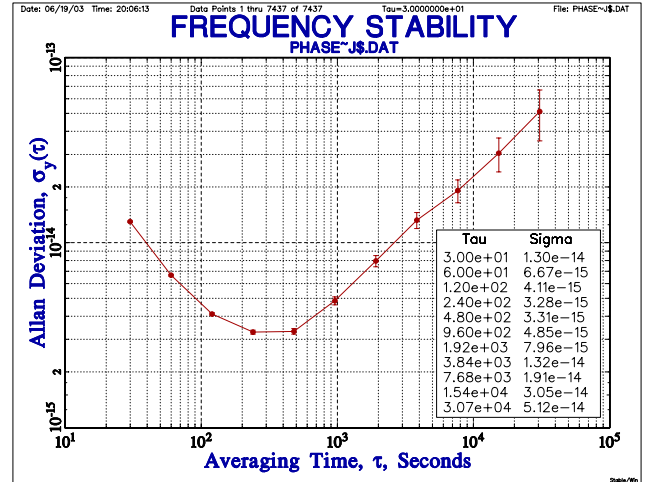


Figure 8. Beat of the sapphire clock with a maser at CNES

For integration times above 200 seconds in figure 8 we see the noise of the sapphire clock. For integration times lower than 200 seconds, we see only the frequency stability of the maser. We can therefore conservatively estimate a frequency stability of order  $10^{-15}$  for 1 second integration times for the sapphire clock, which satisfies the requirements for it to act as a flywheel oscillator for the PHARAO project.

## ACKNOWLEDGMENT

Without the expert design and machining team in the workshop of UWA this work would not have been possible. Thanks to A/Prof. Luiten for invaluable advice and suggestions. Thanks also to the team at CNES for their help in the integration of the clock in Toulouse.

## REFERENCES

- [1] A. J. Giles, A. G. Mann, S. K. Jones, D. G. Blair, and M. J. Buckingham, "A very high stability sapphire loaded superconducting cavity oscillator," *Physica B*, vol. 165, pp. 145-146, 1990.
- [2] S. K. Jones, D. G. Blair, and M. J. Buckingham, "The effects of paramagnetic impurities on the frequency of sapphire loading superconducting resonators," *Electron. Lett.*, vol. 24, pp. 346-347, 1988.
- [3] S. Chang, A. Mann, and A. Luiten, "improved cryogenic sapphire oscillator with exceptionally high frequency stability," *Electron. Lett.*, vol. 36, pp. 480-481, 2000.
- [4] S. Chang, "Ultrastable cryogenic microwave sapphire resonator oscillator," *PhD Thesis University of Western Australia*, 2000.
- [5] A. N. Luiten, A. G. Mann, and D. G. Blair, "Ultra High Q Factor Cryogenic Sapphire Resonator," *IEE Electronics Letters*, vol. 29, pp. 879-881, 1993.
- [6] M. E. Tobar and A. G. Mann, "Resonant Frequencies of High Order Modes in Cylindrical Anisotropic dielectric Resonators," *IEEE Transactions on Microwave Theory and Techniques*, vol. 39, pp. 2077-2083, 1991.
- [7] G. Santarelli, C. Audoin, A. Makdissi, P. Laurent, G. J. Dick, and A. Clarion, "Frequency stability degradation of an oscillator slaved to a periodically interrogated atomic resonator," *IEEE Trans. Utrason. Ferroelect. Freq. Contr.*, vol. 45, pp. 887-894, 1998.
- [8] G. Santarelli, P. Laurent, P. Lemonde, A. Clairon, A. G. Mann, S. Chang, A. N. Luiten, and C. Salomon, "Quantum projection noise in an atomic fountain: A high stability cesium frequency standard," *Phys. Rev. Lett.*, vol. 82, pp. 4619-4622, 1999.
- [9] S. Chang, A. G. Mann, A. N. Luiten, and D. G. Blair, *Phys. Rev. Lett.*, vol. 79, pp. 2141-44, 1997.